



Morphology and enzyme production of *Trichoderma reesei* Rut C-30 are affected by the physical and structural characteristics of cellulosic substrates



Ausra Peculyte^a, George E. Anasontzis^{a,c}, Katarina Karlström^b, Per Tomas Larsson^{b,d}, Lisbeth Olsson^{a,c,*}

^a Department of Chemical and Biological Engineering, Industrial Biotechnology Group, Chalmers University of Technology, SE-412 96 Gothenburg, Sweden

^b Inventia AB, SE-114 86 Stockholm, Sweden

^c Wallenberg Wood Science Center, Chalmers, SE-412 96 Gothenburg, Sweden

^d Wallenberg Wood Science Center, KTH, SE-100 44 Stockholm, Sweden

ARTICLE INFO

Article history:

Received 31 March 2014

Received in revised form 18 July 2014

Accepted 19 July 2014

Available online 2 August 2014

Keywords:

Cellulose I structure

Trichoderma reesei Rut C-30

Submerged cultivation

Biomass degrading enzymes

TMT

Quantitative proteomics

ABSTRACT

The industrial production of cellulolytic enzymes is dominated by the filamentous fungus *Trichoderma reesei* (anamorph of *Hypocrea jecorina*). In order to develop optimal enzymatic cocktail, it is of importance to understand the natural regulation of the enzyme profile as response to the growth substrate. The influence of the complexity of cellulose on enzyme production by the microorganisms is not understood. In the present study we attempted to understand how different physical and structural properties of cellulose-rich substrates affected the levels and profiles of extracellular enzymes produced by *T. reesei*. Enzyme production by *T. reesei* Rut C-30 was studied in submerged cultures on five different cellulose-rich substrates, namely, commercial cellulose Avicel[®] and industrial-like cellulosic pulp substrates which consist mainly of cellulose, but also contain residual hemicellulose and lignin. In order to evaluate the hydrolysis of the substrates by the fungal enzymes, the spatial polymer distributions were characterised by cross-polarisation magic angle spinning carbon-13 nuclear magnetic resonance (CP/MAS ¹³C-NMR) in combination with spectral fitting. Proteins in culture supernatants at early and late stages of enzyme production were labeled by Tandem Mass Tags (TMT) and protein profiles were analysed by liquid chromatography-tandem mass spectrometry. The data have been deposited to the ProteomeXchange with identifier PXD001304. In total 124 proteins were identified and quantified in the culture supernatants, including cellulases, hemicellulases, other glycoside hydrolases, lignin-degrading enzymes, auxiliary activity 9 (AA9) family (formerly GH61), supporting activities of proteins and enzymes acting on cellulose, proteases, intracellular proteins and several hypothetical proteins. Surprisingly, substantial differences in the enzyme profiles were found even though there were minor differences in the chemical composition between the cellulose-rich substrates.

© 2014 The Authors. Published by Elsevier Inc. This is an open access article under the CC BY-NC-SA license (<http://creativecommons.org/licenses/by-nc-sa/3.0/>).

1. Introduction

The filamentous fungus *Trichoderma reesei* is one of the main microorganisms for industrial production of biomass degrading enzymes and in academic research (Diener et al., 2004; Martinez et al., 2008; Percival Zhang et al., 2006; Peterson and Nevalainen, 2012). The hypersecreting mutant strain *T. reesei* Rut C-30, developed after random mutagenesis, exhibits high levels of protein secretion and results in high cellulolytic activity (Montenecourt

and Eveleigh, 1977a,b). Enzyme-aided conversion of cellulose is generally considered to be a sustainable technology for building a sugar platform, which in turn could be converted to a spectrum of products during fermentation processes, with bioethanol being a prime example (Otero et al., 2007).

A number of enzymes with different activities are needed for efficient enzymatic hydrolysis of cellulose (Mansfield et al., 1999; Pauly and Keegstra, 2008; Yang et al., 2011). Among them, cellulases and hemicellulases, which belong to a group of enzymes known as glycoside hydrolases (GH), play an important role in enzymatic hydrolysis of biomass (Dashtban et al., 2009; Lynd et al., 2002; Percival Zhang et al., 2006). Recently a new CAZy class was introduced for enzymes with auxiliary activities, AA9 family in fungi (formerly GH61) (Hemsworth et al., 2014; Horn et al., 2012).

* Corresponding author at: Department of Chemical and Biological Engineering, Industrial Biotechnology Group, Chalmers University of Technology, SE-412 96 Gothenburg, Sweden. Fax: +46 31 772 3801.

E-mail address: lisbeth.olsson@chalmers.se (L. Olsson).

Also, accessory proteins, namely, swollenins (Saloheimo et al., 2002) and expansins (Shcherban et al., 1995) are known to have a beneficial effect on cellulose hydrolysis.

In the natural habitats microorganisms regulate enzyme production for the most efficient usage of the available carbon source (Aro et al., 2005). The ultimate goal in industry is to develop and use natural enzyme producing microorganisms that can produce the target enzymes at high yields and productivity. It has been shown that the source and the chemical composition of biomass have an apparent influence on the secreted enzyme activities in cultures of *T. reesei* Rut C-30 (Alvira et al., 2013; Olsson et al., 2003).

Cellulose, the major polymer in plant cell walls, is a very stable molecule (Wolfenden and Snider, 2001) and it is known to be recalcitrant. The macromolecular structure of cellulose conceals much higher complexity than what would be expected from a polymer composed of linear glucan chains. Cellulose I exists in the form of fibrils, bundles of β -(1,4)-D-glucan polymers. Cellulose I fibrils have species-dependent supramolecular characteristics, such as lateral dimensions. The state of order of the individual polymers in a fibril is highly dependent on their location within the fibril, with surface polymers typically being the least constrained. Depending on the starting material and the isolation procedure used, the cellulose I fibrils can assemble into larger supramolecular structures, fibril aggregates that constitute the cellulose network in e.g. the wood pulp fibre walls after isolation (Hult et al., 2001). This entire porous network has a complex orientation in space. Exposure of the surface area towards enzymatic attack is possibly one of the limiting material properties during enzymatic hydrolysis (Chunilall et al., 2010; Mansfield et al., 1999). Additionally to the complex spatial orientation, it was suggested that cellulose structures have hydrophilic and hydrophobic faces, later showed to be selectively preferred by exocellulase (CBHI) in cellulose hydrolysis (Liu et al., 2011).

Enzyme production is repressed by easily accessible carbon sources, and for the glucose repression deficient strain *T. reesei* Rut C-30, lactose is used as an industrial carbon source. It has been suggested that there is a clear relation between the chemical composition of the substrate used for the fungal growth and the capacity of the produced enzymes to hydrolyse the same substrate (Alvira et al., 2013). So far it has not been attempted to understand how different cellulose-rich substrates affect extracellular enzyme production by the microorganisms.

In the present study, we investigated the hypothesis that the composition of the carbon source used is not the only determining factor affecting the co-regulation of biomass-degrading enzymes (Foreman et al., 2003), but the structural characteristics of the substrate are also important. We expected this influence to be reflected in the profile of the secreted proteins. The major driving force in the present study was to understand how the characteristics such as spatial distributions of fibrils and fibril aggregates, accessible surface area, porosity and particle size influence enzyme production by *T. reesei* Rut C-30. We used five different cellulosic substrates as carbon and energy source in submerged culture experiments: (a) Avicel[®], a commercial cellulose preparation, (b) three industrial-like cellulose-rich pulp substrates which mainly consisted of cellulose, but also contained residual hemicellulose and lignin, and (c) nanocrystalline cellulose (NCC) particles which were made from one of the pulps. The chosen pulp substrates aim at mimicking a commercial 'best possible practise' pulps. The NCC particles were included to assess the possible influence of the fibre wall morphology. Extracellular enzyme production by *T. reesei* Rut C-30 was investigated at the early and late stages of protein production for each substrate using proteomic approach which allowed us to study proteins present even at low amounts. In addition, the chemical and structural properties of the substrates were

determined. Hereby, we linked the physical and structural features of cellulose-rich substrates with the induction of distinct enzyme groups.

2. Materials and methods

2.1. Preparation of substrates

Softwood biomass, an industrially chipped and screened mixture of 40% Scots pine (*Pinus sylvestris*) and 60% Norway spruce (*Picea abies*), was used for the preparation of the substrates, namely pre-hydrolysis soda (PHS), oxygen delignified pre-hydrolysis soda (OPHS) and oxygen delignified pre-hydrolysis kraft (OPHK) pulps. Pre-hydrolysis with water, i.e. autohydrolysis was applied for removal of hemicelluloses prior to the alkaline delignification in soda and kraft pulping. Oxygen delignification in one step was performed in both cases. The lignin content, the sum of acid-insoluble (Klason lignin) and acid soluble lignin, were in PHS pulp around 3% and in the resulting oxygen delignified pulps (OPHS, OPHK pulps) around 1%. The details about the preparation of the pulp substrates are provided in Appendix A Section A.1. The nanocrystalline cellulose (NCC) particles were prepared from OPHS pulp. Avicel[®] served as a reference (Table 1).

2.2. Production of nanocrystalline cellulose

Nanocrystalline cellulose (NCC) particles were produced from OPHS pulp with the application of hydrochloric acid (HCl) hydrolysis. Firstly, around 10 g (dry weight) of never-dried OPHS pulp at 28% dry content was submerged into deionised water (DI) and stirred mildly until the pulp slurry became homogeneous. Then the pulp slurry was filtered through Miracloth (Calbiochem, California, USA). Five hundred mL of 2.5 M HCl were added in a round bottom flask submerged in a container filled with polyethylene glycol (PEG) 200 and connected to a coil condenser, under continuous stirring and heating to 100 °C. The filtered pulp was submerged into the acid. Hydrolysis was performed for 17 h. At the end of the hydrolysis a pinch of sodium chlorite (NaClO₂) was added. After a few minutes of stirring, the entire hydrolysis solution was mixed with approximately 4 L DI water and kept still for approximately one day in room temperature until a sediment of NCC was formed. The supernatant of the sediment was carefully replaced with DI water a few times, until its pH became the same as DI water, pH 7.0. NCC particles were stored in room temperature in DI water.

2.3. Characterisation of the substrates prior to the fungal growth experiments

2.3.1. Characterisation of the fibre wall nanostructures

A CP/MAS ¹³C-NMR method was used for characterisation of the fibre wall nanostructure dimensions. The software for spectral fitting was developed at Innventia AB and is based on a Levenberg-Marquardt algorithm (Larsson et al., 1997). All computations were based on integrated signal intensities as obtained from the spectral fitting (Wickholm et al., 1998). Cellulose I specific surface area was calculated from the lateral fibril aggregate dimensions by assigning a density of 1500 kg m⁻³ to cellulose I (Chunilall et al., 2010). More specifically, the Lateral Fibril Aggregate Dimensions (LFAD), Lateral Fibril Dimensions (LFD), Specific Surface Area (SSA) and crystallinity were determined.

2.3.2. Analysis of ash-content and extractives

Ash-content of biomass and pulps was determined according to ISO 1762. The biomass and pulps were extracted by acetone prior

Table 1
Description of the substrates used in the study.

Abbreviation	Full name	Physical properties	Size	Treatment	Origin
Avicel® PH-101	Commercial microcrystalline cellulose	Dried powder	Micro	Acid hydrolysis of hardwood	Purchased
NCC	Nanocrystalline cellulose	Never-dried particles	Micro and nano	Acid hydrolysis of OPHS	This study
PHS	Pre-hydrolysis soda pulp	Never-dried pulp fibres	Milli (in length)	Pre-hydrolysis soda pulp without bleaching	This study
OPHS	Oxygen delignified pre-hydrolysis soda pulp	Never-dried pulp fibres	Milli (in length)	Oxygen delignification of PHS pulp	This study
OPHK	Oxygen delignified pre-hydrolysis kraft pulp	Never-dried pulp fibres	Milli (in length)	Oxygen delignification of pre-hydrolysis kraft pulp	This study

to analysis of carbohydrates and lignin to determine the amount of extractives according to SCAN-CM 49:03.

2.3.3. Analysis of carbohydrates

Samples were hydrolysed at 121 °C in an autoclave with 0.4 M H₂SO₄, according to SCAN-CM 71:09. The solubilised monosaccharides were quantified using high performance anion exchange chromatography Dionex ISC-5000 system coupled to a CarboPac PA1 (250 mm × 4 mm i.d.) column (Dionex, Sweden) and a pulsed amperometric detector (HPAEC-PAD). Xylan, (galacto)glucomanan and cellulose contents were estimated from the relative carbohydrate composition and non-carbohydrate content for the wood chips used in production of substrates, as previously described (Janson, 1974).

2.3.4. Lignin analysis

After the sulphuric acid hydrolysis described above, the samples were filtered, the acid-insoluble lignin (Klason lignin) was determined gravimetrically according to TAPPI T 222 om-02, and the acid-soluble lignin was measured by UV spectrophotometry at 205 nm according to TAPPI UM 250. MilliQ water was used as a blank and for the dilution of hydrolysate. The content of acid-soluble fraction was calculated using the absorption coefficient value of 110 L g⁻¹ cm⁻¹. The total content of lignin was assumed to be the sum of the amount of acid-soluble and acid-insoluble fraction. Samples were analysed in duplicates.

2.3.5. Water retention value

This analysis estimates the ability of fibres to absorb water and swell. The measurement was done according to SCAN-C 62:00 with minor modifications. In brief, 4 g of pulp was swollen in DI water while stirring until homogeneity. Centrifugal filters (Ultrafree-CL, Millipore, Massachusetts, USA) were filled with the wet pulp and centrifuged at 5000g for 30 min at 25 °C. After the centrifuging the weight of the pulp was recorded and then the pulp was dried at 110 °C for 4 h. The determination was performed in triplicates.

Mini-Water Retention Value (mini-WRV) was calculated according to the expression:

$$WRV = \frac{m_w}{m_s},$$

where m_w is the mass of water; and m_s is the mass of dried pulp.

2.3.6. Pore size determination

Pore size was calculated accordingly (Larsson et al., 2013):

$$t \approx \frac{WRV}{\sigma \phi_L},$$

where t is the half the average pore size; WRV is the water retention value; σ is the specific surface area, value taken from CP/MAS ¹³C-NMR measurements; and ϕ_L is the water density.

The measure $2t$ is the value reported as average pore size. The value $2t$ is comparable to an average pore diameter although this

method does not depend on any particular pore geometry (Larsson et al., 2013).

2.4. Strain, medium and culture conditions

T. reesei Rut C-30 (also designated as NRRL 11460 or ATCC 56765) strain was used in the culture experiments. Spores were propagated on potato dextrose agar (PDA) (Fluka Chemie, Buchs, Switzerland) plates at 30 °C for 7 days from glycerol solution stocks (stored at -80 °C). The PDA medium was supplemented with 1 mL trace element solution per L of medium. The trace element solution was composed of 1 g ZnSO₄·7H₂O and 0.5 g CuSO₄·5H₂O in 100 mL MilliQ water.

Spores were harvested by adding 10 mL MilliQ water on a PDA plate of *T. reesei* Rut C-30 and scraping the plate with a sterile spatula. The spore solution was filtered through three layers of Miracloth (Calbiochem, California, USA) and counted under a light microscope using an improved Neubauer chamber.

Batch cultures were performed in duplicates in 1 L working volume in Infors HT 3.6 L bioreactors (Labfors 3 and 4, Bottmingen/Basel, Switzerland) equipped with two oblique blade impellers with six blades. The temperature was set to 26 °C, the aeration rate to 0.9 vvm and the agitation to 400 rpm. The pH was maintained at 4.5 by addition of either 1 M NaOH or 1 M HCl.

Bioreactors were inoculated to a final concentration of 2×10^9 spores L⁻¹. The cultivation medium was composed of (per L): 4 g KH₂PO₄, 13.6 g (NH₄)₂SO₄, 0.8 g CaCl₂·2H₂O, 0.6 g MgSO₄·7H₂O, 10 mg FeSO₄·7H₂O, 3.2 mg MnSO₄·H₂O, 2.8 mg ZnSO₄·7H₂O, 4 mg CoCl₂·6H₂O, 6 g bacto peptone (BD, New Jersey, USA), 100 µL anti-foam 204 (AB Nijmegen, Nijmegen, The Netherlands) (Lehman, 2011). Carbon source was added yielding a final concentration of 16–20 g L⁻¹ cellulose. Prior to *T. reesei* Rut C-30 cultivations substrates were autoclaved and it was confirmed by CP/MAS ¹³C-NMR that autoclaving did not alter the structure of cellulose (data not shown). As carbon sources, we utilised Avicel® PH-101 (Fluka BioChemika, Ireland) and the following softwood pulps: PHS, OPHS and OPHK, and NCC particles produced from OPHS pulp.

Culture samples of 10 mL were harvested every day by centrifugation; they were filtered through a 0.22 µm Nylon filter and the supernatants were stored at -20 °C. The samples were analysed for protein concentrations and enzyme activities. Possible losses of enzymes from the culture supernatants due to their productive and non-productive adsorption to the substrates were not investigated because we made an assumption that despite all possible adsorption, the free enzymes composition would be informative enough.

2.5. Enzyme activity measurements

Filter paper activities in the supernatants were determined in 96-well microtitre plates (Xiao et al., 2004). The plates were sealed and incubated in a water bath. Glucose was used for the standard curve. One filter paper unit (FPU) was defined as the amount of

enzyme releasing 1 μmol of reducing sugar from Whatman filter paper grade No.1 per 1 min. Technical replicates were measured on each supernatant and FPU values were calculated from the average values of the replicate measurements.

Endo- β -1,4-glucanase activity was determined according to the carboxymethyl cellulose (CMC) assay (Ghose, 1987). All volumes were reduced 17 times to fit the reaction in the 96-well microtitre plates. Glucose was used for the standard curve. One unit (IU) was defined as the amount of enzyme releasing 1 μmol of reducing sugar from CMC per 1 min. Technical replicates were measured on each supernatant and IU values were calculated from the average values of the replicate measurements.

2.6. Protein measurements

Proteins from the supernatants were quantified by using the commercial Bio-Rad protein assay kit which is based on the method of Bradford (Bradford, 1976) using bovine serum albumin as a standard. The assay was performed in 96-well microtitre plates in duplicates for each sample. The protein concentration was defined as the amount of extracellular proteins measured per 1 L of culture supernatant.

The supernatant proteins were separated by sodium dodecyl sulphate polyacrylamide gel electrophoresis (SDS–PAGE) in denaturing conditions (Laemmli, 1970) in the molecular weight range 15–170 kDa.

2.7. Proteomics analysis of the supernatants

Quantitative proteomics analysis from the supernatants of the cultures was performed using liquid chromatography–tandem mass spectrometry (LC–MS/MS) and labeling the proteins with Tandem Mass Tag (TMT)[®] (Thermo Scientific, Basel, Switzerland) (Thompson et al., 2003). Proteomics analysis was done on 15 supernatant samples from the different cultivations, consisting of early and late samples of the protein production. Samples were withdrawn from each cultivation and analysed (more explanations are given in Results part, Section 3.5). Three sets of 6-plex TMT compounds were used to analyse all 15 supernatants. Each set had 5 different samples from the cultivations and one sample from the pool, which consisted of equal amounts (by weight) of proteins from all the 15 samples.

All materials were obtained from GE Health Care Life Science (Uppsala, Sweden) unless otherwise stated. Eighteen m Ω water was produced using the MilliQ water purification system (Millipore, Billerica, MA).

2.3.7. Protein labeling with TMT and LC–MS/MS analysis

Protein sample preparation before TMT labeling, the procedure of TMT labeling of proteins and LC–MS/MS analysis is described in detail in Appendix A Section A.2.

2.3.8. Database search

MS raw data files for each TMT set were merged for relative quantification and identification using Proteome Discoverer version 1.3 (Thermo Fisher Scientific, Inc., Waltham, MA, USA). A database search for each set was performed with the Mascot search engine (Matrix Science Ltd., London, United Kingdom) using *T. reesei* V2 ‘filtered models’ protein database obtained from the Joint Genome Institute website (<http://genome.jgi.doe.gov/Trire2/Trire2.download.html>, Department of Energy, Joint genome institute, CA, USA) (Martinez et al., 2008). MS peptide tolerance was 5 ppm and MS/MS tolerance of 100 molecular mass units. Tryptic peptides were accepted with one missed cleavage and variable modifications of methionine oxidation, cysteine methylthiolation and fixed modifications of N-terminal TMT6plex and lysine TMT6plex were selected.

An exclusion list of *m/z* values was generated from the search results whereby only peptide spectral matches accepted at 1% False Discovery Rate (FDR) were included, with a mass tolerance of 5 ppm. For the exclusion list, the retention time window was set to 2 min. The sample was re-injected into the Q Exactive mass spectrophotometer (Thermo Fisher Scientific, Inc., Waltham, MA, USA) interfaced with an in-house constructed nano-LC column and run as with the exclusion list using the same parameters as in the first MS analysis. The MS raw files from the first and second MS analysis were combined and searched as described above and a second exclusion list was generated with the same settings as previously described. The TMT sample was re-injected for a third run using the second exclusion list and MS analysis was performed with the same parameters as first and second analysis. The three MS raw data files were combined and searched as described above.

2.3.9. TMT quantification

The detected peptide threshold in the software was set to 1% or 5% FDR by searching against a reversed database and the result was filtered by selecting proteins with at least one unique peptide per protein. Identified proteins were grouped by sharing the same sequences to minimise redundancy. For TMT quantification, the ratios of the TMT reporter ion intensities in MS/MS spectra ($[M+H]^+$ *m/z* 126–131) from raw data sets were used to calculate fold changes between samples. Ratios were derived by Proteome Discoverer version 1.3 using the following criteria: fragment ion tolerance as 50 ppm for the most confident centroid peak. TMT reagent purity correction factors were used and missing values were replaced with minimum intensity. Only peptides unique for a given protein were considered for relative quantification, excluding those common to other isoforms or proteins of the same family. The quantification was normalised using the protein median with a minimum protein count of 20. Peptides with co-isolation of greater than 30% were rejected for quantification purposes. The results were then exported into MS Excel (Microsoft, Redmond, WA) for further data interpretation and statistical analysis.

2.3.10. Assignments of protein names

The search for the protein functions was done in JGI Genome Portal using the protein ID numbers and searching for the protein names/functions in *T. reesei* database <http://genome.jgi.doe.gov/Trire2/Trire2.download.html>. Proteins that did not have assigned names were grouped as hypothetical.

2.8. Microscopy

Throughout the cultivation culture morphology was monitored offline using inverted fluorescence microscope Leica DMI4000B (Leica Microsystems, Heerbrugg, Switzerland) equipped with a Leica DFC360 FX high speed fluorescence camera. A drop of culture was applied on a microscope slide and covered with a slip. The images were acquired at 100 \times magnification.

3. Results

In the present work, we aimed at evaluating the influence of factors such as; chemical composition, physical properties, supra-molecular structure, pore sizes and accessible surface area of five different cellulose-rich substrates to the production of enzyme mixtures with distinct profiles by fungus *T. reesei* Rut C-30. The fungus was cultivated in submerged cultures where these five cellulose-rich substrates were used as carbon and energy sources. Identification and quantification of the proteins in the culture supernatants by proteomics analysis showed certain enzymes to be more abundant and we discussed the possible correlation between the characteristics, chemical and structural, of the substrates.

3.1. Characterisation of the substrates

To understand how levels and profiles of enzymes produced by fungus *T. reesei* Rut C-30 are affected by different physical and structural properties of cellulose, five cellulose-rich substrates, namely, commercial cellulose Avicel®, nanocrystalline cellulose (NCC) particles and three industrial-like pulp substrates were evaluated in the submerged cultivations (Table 1).

The spatial polymer distributions and crystallinity were analysed by CP/MAS ¹³C-NMR and their pore sizes were calculated (Table 2).

All substrates consisted primarily of cellulose, with only minor amounts of hemicelluloses and lignin. There were less than 2.5 mg g⁻¹ extractives in the pulps (Table 3). Avicel® is a commercial microcrystalline cellulose, originating from hardwood were the relative carbohydrate composition was determined to be composed of 96.8% glucose, 2.2% xylose, 0.9% mannose, <0.1% arabinose and <0.1% galactose.

3.2. Cultivation experiments on Avicel® and three different pulps

During the fungal cultivations on Avicel®, proteins were detected in the supernatants after 30 h and a continuous increase was observed throughout the cultivations, reaching 2 g L⁻¹ of total protein concentration, based on the measurements according to the Bradford assay. During the cultivations on the pulp substrates, proteins were not detected in the supernatants until after 130 h of cultivation. The total protein concentration became constant after around 170 h of cultivation, reaching values around 0.4 g L⁻¹, which was five times lower than in the cultivations on Avicel® (Fig. 1A).

Filter paper assay (FPA) results followed the same pattern as the protein concentrations. The highest filter paper units (FPU) were measured in the cultivations on Avicel® (3.5 FPU mL⁻¹). The highest FPU on the pulps and NCC were 14 times lower than that on Avicel®, i.e. 0.25 FPU mL⁻¹ (Fig. 1B). Specific filter paper activities were constant during the fungal cultivations on NCC, PHS, OPHS and OPHK, reaching 0.6, 0.7, 0.8 and 0.3 FPU mg⁻¹, respectively. During the fungal cultivation on Avicel®, a continuous increase from 0.6 to 1.9 FPU mg⁻¹ was observed.

Endo-β-1,4-glucanase activity had also the same trend as protein measurements and filter paper activity. The highest endoglucanase activity was in the cultivations on Avicel® (21.7 IU mL⁻¹). The highest endoglucanase activities in the cultures on the pulps and NCC were 2–5 times lower compared to the cultures on Avicel® (Fig. 1C and Appendix B Fig. B.1).

The cultivation experiments for each fungal growth condition were done twice and showed the same pattern; the protein titres, filter paper activity and endoglucanase activity measurements for both experiments are shown in the Appendix B Fig. B.1.

Table 2
Structural characteristics of the substrates used in the study.

Substrate	LFD (nm)	LFAD (nm)	SSA (m ² g ⁻¹)	Cr (%)	Pore size (nm)
Avicel®	4.5 ± 0.1	23.7 ± 1.1	113 ± 5	56 ± 3	n.a.
NCC	5.6 ± 0.2	28.9 ± 1.7	92 ± 5	63 ± 2	n.a.
PHS	4.5 ± 0.1	19.1 ± 1.3	140 ± 10	56 ± 2	21 ± 1
OPHS	4.7 ± 0.1	17.5 ± 0.8	153 ± 7	57 ± 1	18 ± 1
OPHK	4.7 ± 0.1	19.2 ± 0.6	139 ± 5	58 ± 2	19 ± 1

LFD – Lateral Fibril Dimension (or fibril thickness); LFAD – Lateral Fibril Aggregate Dimension (or aggregate thickness); SSA – Specific Surface Area; Cr – total crystallinity; n.a. – not analysed; errors – the precision of the NMR spectral fitting is expressed as a standard error of the mean in LFD, LFAD, SSA and Cr calculations; error values in pore size measurements represent min and max values of the mean of two replicates.

Table 3
Chemical composition (%) of the used substrates, originating from softwood.

Sample	PHS	OPHS	NCC	OPHK
Acid-insoluble lignin	2.4	0.5	<0.5	1.2
Acid-soluble lignin	0.5	0.5	<0.5	0.5
Extractives	<0.3	n.a.	n.a.	<0.1
Ash content	<0.1	<0.2	n.a.	n.a.
Xylan	1.5	1.5	0.8	1.8
(Galacto)glucomannan	1.0	0.9	1.0	1.3
Cellulose	94.6	96.6	97.2	95.2

n.a. – not analysed.

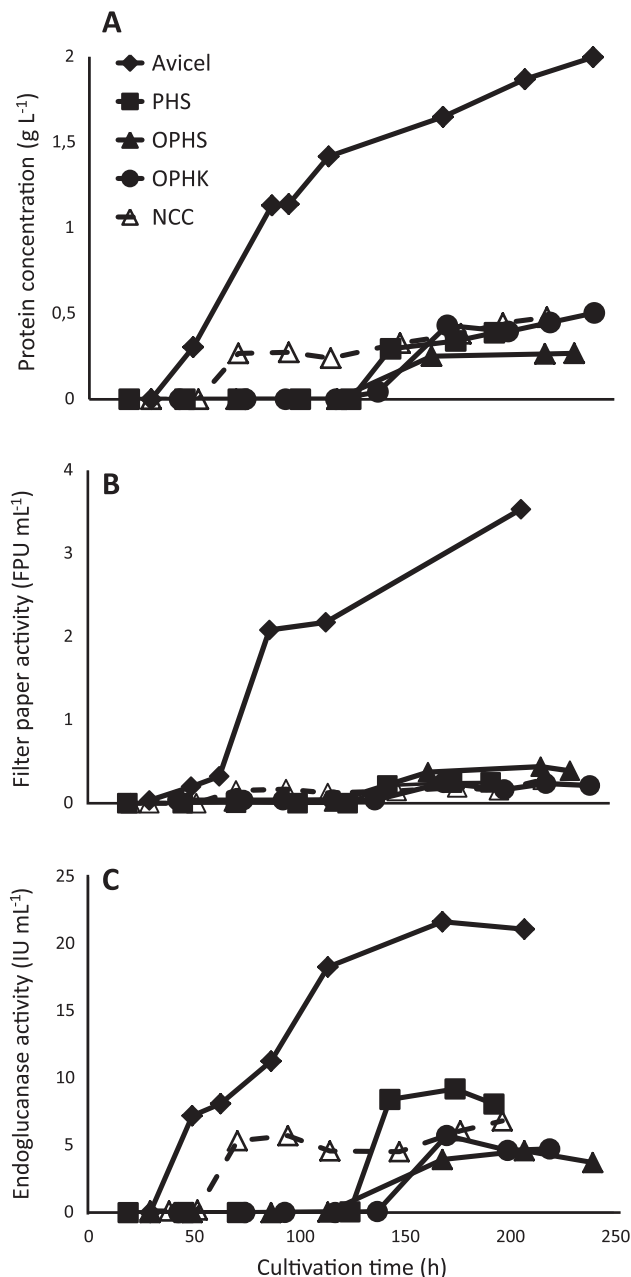


Fig. 1. Total protein concentrations ($\text{g}_{\text{proteins}}/\text{L}_{\text{culture supernatant}}$) (A), filter paper activities (FPU mL^{-1}) (B) and endoglucanase activities (IU mL^{-1}) (C) of *T. reesei* Rut C-30 batch cultivations on the following carbon sources: Avicel® (◆), PHS (■), OPHS (▲) and OPHK (●) and NCC (△).

3.3. Effect of particle size on enzyme production

In order to evaluate if reduction of particle size of the pulps (particle length in milli scale) to the particle size of Avicel® (particle size in micro scale) has an influence on protein production, we performed acid hydrolysis on OPHS pulp generating NCC particles. Evaluation under the microscope revealed that NCC particles were a mixture of micro- and nano-sizes (data not shown). The size of NCC particles and their chemical composition became similar to that of Avicel® (Tables 1 and 3).

Although proteins were detected in the supernatant of the NCC culture earlier than on OPHS (50 h compared to 118 h on OPHS), it was still later than on Avicel® (30 h). The total protein concentration measured in the cultures on NCC particles followed the same pattern that was observed in all fungal cultures on the pulp fibres: when the plateau was reached, the protein concentration was stable until the end of the cultures. During the fungal growth on NCC, the protein concentration reached a plateau after around 70 h of cultivation, while in the case of OPHS it became stable after 160 h. The highest protein concentration observed during fungal growth on NCC was 0.5 g L^{-1} , i.e. 4 times lower than on Avicel® (2 g L^{-1}) (Fig. 1A).

During the fungal cultivation on NCC particles, filter paper activity followed the same pattern that was observed for the total protein concentration i.e., delayed detection and a stabilisation after about 70 h, while during the growth on Avicel®, filter paper activity was gradually increasing until the end of the culture (Fig. 1B).

3.4. Effect of different carbon sources on fungal morphology

Throughout the cultivations on Avicel® and NCC particles, the morphology of *Trichoderma* remained similar, but the growth on the pulps showed very distinct fungal morphology (Fig. 2 and Appendix B Fig. B.2). During the growth on Avicel® and NCC, fungal hyphae were homogeneous, thin and septa were not so distinct (Fig. 2A–D). In contrast, in the cultivations on the pulps fungal hyphae were quite thick, with adventitiously formed septa along the hyphae (Fig. 2E and F). Thick and bulbous hyphae were observed during the cultivations on the pulps when the density of fibres in the fermenters was high. But when most of the fibres were hydrolysed, fungal hyphae became more uniform and thinner. Also, during the growth on the pulp fibres, *T. reesei* formed pellets which consisted of hyphae and pulp fibres. When the fibres were hydrolysed, the hyphae were growing in dispersed manner. On the contrary, no pellet formation was observed during fungal growth on Avicel® and hyphal growth was dispersed (Appendix B Fig. B.3).

3.5. Proteomics analysis of the culture supernatants

SDS–PAGE analysis indicated that the protein production pattern differed between the cultivations on different carbon sources (Appendix B Fig. B.4).

Samples from early and late time point of fungal cultures were selected for proteomics analysis. The mass spectrometry proteomics data have been deposited to the ProteomeXchange Consortium (Vizcaíno et al., 2014) via the PRIDE partner repository with the dataset identifier PXD001304 and <http://dx.doi.org/10.6019/PXD001304>. Early samples represent the time point when proteins were first detected by Bradford method (Avicel® 50 and 53 h, NCC 71 h, PHS 144 h, OPHS 163 and 169 h and OPHK 171 h). Late samples represent late stages in protein production aiming at similar time points for all the cultures (Avicel® 195 and 208 h, NCC 218 h, pulps PHS 193 h, OPHS 208 and 217 h and OPHK 220 h). As equal amounts of total proteins from the culture supernatants

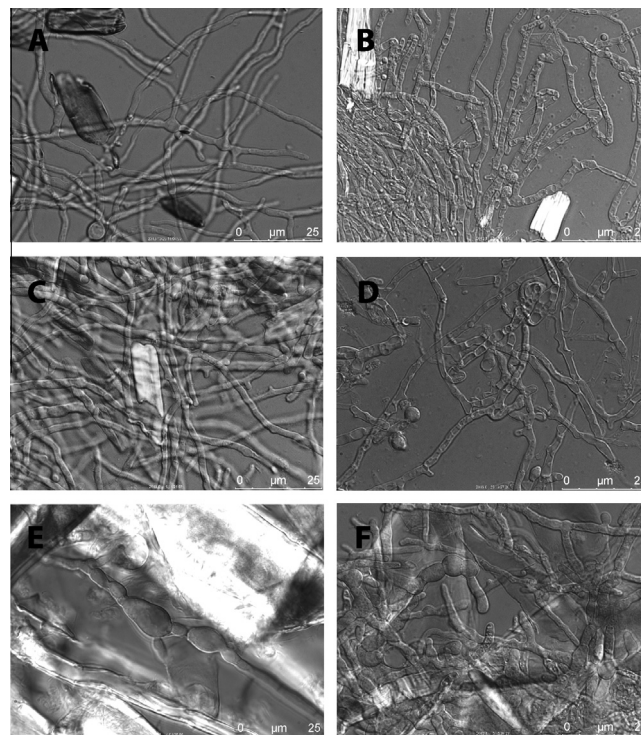


Fig. 2. Microscope pictures of *T. reesei* Rut C-30 cultures on Avicel® at 52 h (A) and 114 h (B), NCC at 52 h (C) and 95 h (D), and OPHS at 87 h (E) and 114 h (F).

were analysed, therefore the comparison of the proteomics data shows compositional changes in the samples.

We evaluated if the afore mentioned differences between growth on the different carbon and energy sources, indicate a different physiological state of the microorganism in respect to the structure of cellulose, which is also reflected on the extracellular enzymes secreted. Therefore, the culture supernatant samples from early and late stages of protein production were labeled with TMT and analysed by LC–MS/MS. In total 124 proteins were identified and quantified and among them 25 proteins were overlapping in every sample. Overall, 99 proteins were detected in set A, 64 in set B and 40 in set C (Appendix C Table C.1). Proteins were classified according to their function into 8 groups: hydrolysis of (a) cellulose, (b) hemicellulose and other polysaccharides, (c) other glycoside hydrolases, (d) lignin degradation, (e) supporting activities, (f) proteases/peptidases, (g) intracellular and membrane bound proteins and (h) hypothetical proteins.

For each carbon source, late samples were compared with their respective early one: there were no new proteins measured in the late samples compared to the early but quantities of the certain proteins were different and 10 proteins were in common in every culture (Fig. 3). Repeated growth experiments showed the same tendency (Appendix B Table B.1).

Fig. 4 depicts the fold differences of the common proteins in the late cultures on NCC, PHS, OPHS and OPHK compared to Avicel®.

4. Discussion

Until now, low protein titres were achieved during cultivation on biomass compared to cultivations on lactose, which is traditionally used in industry for enzyme production. This suggests that characteristics of the biomass and its major component, cellulose, influence the enzyme production. Cellulose is much more complex than just being a polymer composed of linear glucan chains. To

Involved in cellulose hydrolysis		Avicel	NCC	PHS	OPHS	OPHK
Trire2 72567	CBH2 (Cel6)	13	10			
Trire2 123989	CBH1 (Cel7A)	3	6	3		
Trire2 122081	EG1 (Cel7B)		6			2
Trire2 76672	β -glucosidase (Cel3A)	2	12	-2		
Hydrolysis of hemicellulose/other polysaccharides						
Trire2 82235	α -glucosidase	-5	-2	-4	-2	
Trire2 111849	Xylanase 4		9			
Supporting activities						
Trire2 123992	Swollenin	4	2		-3	
Trire2 73643	EG4 (Cel61A)	4		3		
Trire2 120961	Cel61B	-88	-4	-4		
Trire2 123940	Cip 2	7	2	3		5

A fold decrease  A fold increase 

Fig. 3. Comparison of the fold changes of protein amounts at late stages of protein production to the early in the different cultivations. A fold decrease (negative value) in the different cultivations compared the early sample is indicated by different tones of magenta and a fold increase (positive value) is indicated by different tones of turquoise. Each value represents an average value of the ratio of the late samples versus the average of the early samples of the repeated cultivation experiments. The relative quantities of the proteins which had a fold difference below two are coloured in grey. (For interpretation of the references to color in this figure legend, the reader is referred to the web version of this article.)

Involved in cellulose hydrolysis		NCC	PHS	OPHS	OPHK
Trire2 72567	CBH2 (Cel6)		-6	-4	-8
Trire2 123989	CBH1 (Cel7A)	5			-2
Trire2 122081	EG1 (Cel7B)	5	2		
Trire2 76672	β -glucosidase (Cel3A)	3	-3	-4	-4
Trire2 120312	EG2 (Cel5A)	—		-4	—
Trire2 123232	EG3 (Cel12A)	—			—
Hydrolysis of hemicellulose/other polysaccharides					
Trire2 82235	α -glucosidase	3	6	4	3
Trire2 121127	β -xylosidase		-2		-2
Trire2 72526	α -glucuronidase	-2			
Trire2 49081	Xyloglucanase (Cel74A)	-3	-2		
Trire2 111849	Xylanase 4		-4	-3	-12
Trire2 56996	Endo-1,4- β -mannosidase	-2	-2	-7	-7
Trire2 124175	β -1,3-glucanase	—	6	5	—
Trire2 44214	Axe2	—		3	—
Trire2 123818	Endoxylanase 2	—	-2	-4	—
Trire2 120229	Xylanase 3	—	-11	-11	—
Other glycoside hydrolases					
Trire2 65406	GH16	—	5	4	—
Trire2 69276	GH30	—	-7	-9	—
Trire2 104461	Hydrolase	—	-5	-3	—
Supporting activities					
Trire2 123992	Swollenin	-2	2	-3	-4
Trire2 73643	EG4 (Cel61A)	-3		2	-7
Trire2 120961	Cel61B	14	9	7	23
Trire2 123940	Cip 2	-5		-6	-2
Trire2 73638	Cip1	—			—

A fold decrease  A fold increase 

Fig. 4. The relative quantities of proteins measured in all cultivations at the late stage of the cultivation compared to the late sample of the cultivations with Avicel® as carbon source. A fold decrease (negative value) in the different cultivations compared to Avicel® is indicated by different tones of magenta and a fold increase (positive value) is indicated by different tones of turquoise. Each value represents an average value of the repeated cultivation experiments. The relative quantities of the proteins which had less than twofold difference compared to Avicel® are coloured in grey. Proteins which were not detected in the cultivations with the pulps and NCC compared to Avicel® are indicated as '—'. (For interpretation of the references to color in this figure legend, the reader is referred to the web version of this article.)

evaluate the influence of the complexity of cellulose on enzyme production by *T. reesei* Rut C-30, five different cellulosic substrates were chosen as carbon sources.

To understand why the pulp (PHS, OPHS, OPHK) fibres resulted in 5 times lower protein concentrations than Avicel®, fungal morphology and furthermore the possible relation between the chemical and structural characteristics of the substrates and the profile of the enzymes produced were evaluated. At the start of the cultivations on the respective substrates, the viscosity of the growth media with the pulp fibres, Avicel® and NCC were different; cultures with the pulp fibres were very viscous on the contrary to Avicel® and NCC. Big oxygen bubbles were observed in the cultivations on the pulps at the beginning of the cultures, which showed the difficulty in dispersing the air bubbles which in turn was an indication of oxygen transfer problems. Also, fungal hyphae were thick and bulbous in the cultures on the pulp fibres when the density of the fibres was high which could be a result of oxygen and nutrient transfer limitations due to the high viscosity of the fungal culture broth. Similar morphology has been observed in *A. niger* in manganese deficient media (Papagianni et al., 1999), suggesting that nutrient transfer limitations could be a reason for morphological abnormalities in *T. reesei*. However, at the later stage of the cultivations on the pulps, no bulbous hyphae were observed and the growth medium was considerably less viscous. At that stage of the cultivations, proteins were produced. Contrary to the cultivations on the pulp fibres, fungal hyphae were homogeneous during the growth on Avicel® (microcrystalline cellulose powder) and NCC (particle sizes similar to Avicel®). Consequently, a plausible cause of irregular fungal morphology was mass transfer limitation.

Protein amounts resulting after the growth on NCC were similar to protein concentrations measured after the growth on the pulp fibres. The chemical composition of the substrates had minor differences and is therefore not likely to be the reason for the large difference in the protein concentrations between Avicel® and the pulps or NCC. The different structural characteristics, i.e. LFAD and SSA, of Avicel® compared to the pulps suggest that these could be among the influencing factors for the different amount of proteins produced and enzyme profile in the cultures on Avicel®, compared to the cultures on the pulps. The pulps had similar structural characteristics, namely, LFAD, SSA and crystallinity, among themselves at the start of the cultivations, and also exhibited similar protein concentrations and FPU and endoglucanase activities (Fig. 1) during the fungal growth. For efficient enzymatic hydrolysis of cellulose, the pore sizes should be larger than the sizes of the enzyme molecules (Chandra et al., 2007). An enzyme molecule bound to the cellulose have a projection height around 10 nm (Liu et al., 2011). The average pore sizes of the pulp fibres were nearly two times larger than the size of the enzymes. If we take enzyme size of 10 nm as the representative one of the average enzyme sizes, then all surfaces of the pulp fibres were theoretically available for the enzymes. The pore method used (Larsson et al., 2013) was incapable of measuring average pore sizes on samples lacking fibre wall morphology, such as the 'powder' (Avicel®) and the 'particle' (NCC). The NCC substrate can be viewed as a pulp with very large pores. No pore system restricts access of the enzymes to the surface area present because less ordered structures have been removed by the acid hydrolysis during manufacture of NCC particles. This may explain the early increase in protein concentration observed for the NCC in Fig. 1. On the contrary, Avicel® consists of larger and dried during preparation particles. Drying is a process known to irreversibly decrease pore sizes and specific surface area of cellulose rich particles (Esteghlalian et al., 2001; Hult et al., 2001). Avicel® is known to be a recalcitrant substrate for enzymes (Qing and Wyman, 2011). As a consequence, *T. reesei* exhibited a different enzyme profile for the hydrolysis of Avicel® than for hydrolysis of the pulp fibres or NCC particles.

T. reesei secretes two CBHs, CBH1 and CBH2, which hydrolyse crystalline cellulose into cellobiose (Igarashi et al., 2011; Teeri,

1997). The last step in complete hydrolysis of cellulose requires β -glucosidase which is responsible for the conversion of cellobiose into two glucose molecules. Samples from the early time point and the late time point of fungal cultures were selected for proteomics analysis in order to understand if *T. reesei* Rut C-30 during the time course of the cultivations exhibited different secreted enzyme profiles as a response to the different cellulose-rich substrates. Among the proteins in common there were only small changes in the abundance of proteins in early and late samples of fungal growth on the pulp fibres. On the contrary, the fungal cultures on Avicel[®] and NCC exhibited a greater variation in protein amounts in early and late samples. Noticeably, there was an increase of cellulases CBH2, CBH1, EG1 and β -glucosidase at the late stage of protein production during the fungal growth on NCC. It was noted that during the fungal growth on Avicel[®], the highest amount of CBH2 was found in the late sample and there was no difference in EG1 amount in the late sample. Increased amounts of swollenin and Cip2 during the fungal growth on Avicel[®] in the late sample possibly aided in increasing the accessibility of cellulose to other enzymes. A decrease of Cel61B during the fungal growth on PHS, NCC and especially on Avicel[®] was observed, which could be the result of non-productive adsorption or degradation of proteins due to proteolytic activity.

Comparison of the proteomics data of the late samples of the fungal growth on the pulps and NCC to the late cultures on Avicel[®] (Fig. 4) showed significant differences in protein profiles. These results suggest that the co-regulation of biomass-degrading enzymes on the transcriptional level due to the composition of the carbon source used (Foreman et al., 2003) is not the only determining factor. The structure of cellulose plays a very important role. However, possible structural changes of the substrates at the end of the cultivations cannot be measured because for CP/MAS ¹³C-NMR analysis a substantial amount of relative pure cellulosic substrate is needed which is not possible to obtain from fungal biomass matrix during the cultivations.

It has been shown that lignin cause steric hindrance of cellulose and non-productive adsorption of cellulases (Berlin et al., 2006). However, in our study the amount of lignin present did not have any influence on protein production because the same amounts were determined during the growth on the pulps which contained 1% and 3% of lignin.

Two enzymes from AA9 family (formerly GH61) (Hemsworth et al., 2014; Horn et al., 2012), Cel61A (Trire2 73643) and Cel61B (Trire2 120961), were found in detectable amounts during the growth on all five substrates. Cel61B was more abundant in all the cultivations compared to Avicel[®] but Cel61A had lower abundance in NCC and OPHK. Differences in the structures, Cel61A has a carbohydrate-binding module (CBM) whereas Cel61B has no CBM (Karkehabadi et al., 2008), suggested that these enzymes have different binding capacity to cellulose.

Swollenin (Trire2 123992), a non-hydrolytic protein which has been shown to increase cellulase efficiency, was detected in higher amounts in the cultures with Avicel[®] compared to the other substrates. Higher amounts of swollenin in Avicel[®] cultures could have aided the degradation of cellulose by disrupting the crystalline structure and improving the accessibility of cellulose for the hydrolytic enzymes.

T. reesei is known to produce high levels of proteases (Zhang et al., 2014). There were proteases measured in all cultivations which most likely were produced due the peptone added into the growth medium as nitrogen source. In plant cell walls, however, proteins are known to play a critical role during plant development and adaptation to the environment (Albenne et al., 2013). Therefore, protease secretion by the microorganism would aid in biomass degradation. The substrates used in this study underwent

a pretreatment step, so it is not likely that proteins would still be present in the cell walls of the substrates.

A considerable list of hypothetical proteins indicated that many enzyme activities are still not known. Among these hypothetical proteins there could be some proteins which have a role in cellulose degradation.

5. Conclusion

T. reesei is the most commonly used filamentous fungus in enzyme industry and academic research for production of cellulolytic and hemicellulolytic enzymes for hydrolysis of biomass. In this study we investigated the influence of five different cellulose-rich substrates on the enzyme production by *T. reesei* Rut C-30. Substantial differences in the extracellular enzyme profiles between the fungal cultures grown on Avicel[®], NCC and three different pulp substrates, respectively, were observed. Structural differences of the cellulose-rich substrates were the defining factors which caused *T. reesei* to exhibit different extracellular enzyme profiles in the respective cases. A partial explanation for the extracellular enzyme profile may be that cellulose-rich substrates were never-dried, contrary to Avicel[®]. Drying is known to cause structural changes. Comparison of the culture supernatants with proteomics tools at the early and late stage of protein production indicated that there were no qualitative differences between the samples, but only quantitative; fungal cultures from growth on Avicel[®] and NCC showed a greater variation. There were only minor differences in the chemical composition of the substrates, which consisted primarily of cellulose (95–97%) and varied amounts of hemicelluloses and lignin. We showed that the chemical differences were not the main cause for the different enzyme profiles exhibited by the fungus. Morphological abnormalities were observed during the fungal growth on the pulp fibres which most likely were caused by mass transfer limitations due to the viscosity of the growth media.

Acknowledgments

The authors would like to thank Diarmuid Kenny and Carina Sihlbom from The Proteomics Core Facility at Sahlgrenska Academy, University of Gothenburg for the proteomics analysis by TMT labeling and LC-MS/MS, and also for the help to analyse mass spectrometry results. We also thank Fredrik Aldaeus from Innventia AB, Stockholm for the discussions of the results. This work was funded by Swedish Research Council VR under the scheme for strategic energy research (No. 621-2010-3788).

Appendices

Supplementary data associated with this article can be found, in the online version, at <http://dx.doi.org/10.1016/j.fgb.2014.07.011>.

References

- Albenne, C., Canut, H., Jamet, E., 2013. Plant cell wall proteomics: the leadership of *Arabidopsis thaliana*. *Front. Plant Sci.* 4, 111.
- Alvira, P., Gyalai-Korpos, M., Barta, Z., Oliva, J.M., Réczey, K., Ballesteros, M., 2013. Production and hydrolytic efficiency of enzymes from *Trichoderma reesei* RUTC30 using steam pretreated wheat straw as carbon source. *J. Chem. Technol. Biotechnol.* 88, 1150–1156.
- Aro, N., Pakula, T., Penttilä, M., 2005. Transcriptional regulation of plant cell wall degradation by filamentous fungi. *FEMS Microbiol. Rev.* 29, 719–739.
- Berlin, A., Balakshin, M., Gilkes, N., Kadla, J., Maximenko, V., Kubo, S., Saddler, J., 2006. Inhibition of cellulase, xylanase and beta-glucosidase activities by softwood lignin preparations. *J. Biotechnol.* 125, 198–209.
- Bradford, M.M., 1976. A rapid and sensitive method for the quantitation of microgram quantities of protein utilizing the principle of protein-dye binding. *Anal. Biochem.* 72, 248–254.

- Chandra, R.P., Bura, R., Mabee, W.E., Berlin, A., Pan, X., Saddler, J.N., 2007. Substrate pretreatment: the key to effective enzymatic hydrolysis of lignocellulosics? *Adv. Biochem. Eng. Biotechnol.* 108, 67–93.
- Chunilall, V., Bush, T., Larsson, P.T., Iversen, T., Kindness, A., 2010. A CP/MAS ¹³C-NMR study of cellulose fibril aggregation in eucalyptus dissolving pulps during drying and the correlation between aggregate dimensions and chemical reactivity. *Holzforschung* 64, 693–698.
- Dashtban, M., Schraft, H., Qin, W., 2009. Fungal bioconversion of lignocellulosic residues; opportunities & perspectives. *Int. J. Biol. Sci.* 5, 578–595.
- Diener, S.E., Chellappan, M.K., Mitchell, T.K., Dunn-Coleman, N., Ward, M., Dean, R.A., 2004. Insight into *Trichoderma reesei*'s genome content, organization and evolution revealed through BAC library characterization. *Fungal Genet. Biol.* 41, 1077–1087.
- Esteghlalian, A.R., Bilodeau, M., Mansfield, S.D., Saddler, J.N., 2001. Do enzymatic hydrolyzability and Simons' stain reflect the changes in the accessibility of lignocellulosic substrates to cellulase enzymes? *Biotechnol. Prog.* 17, 1049–1054.
- Foreman, P.K., Brown, D., Dankmeyer, L., Dean, R., Diener, S., Dunn-Coleman, N.S., Goedegebuur, F., Houfek, T.D., England, G.J., Kelley, A.S., Meerman, H.J., Mitchell, T., Mitchinson, C., Olivares, H.A., Teunissen, P.J., Yao, J., Ward, M., 2003. Transcriptional regulation of biomass-degrading enzymes in the filamentous fungus *Trichoderma reesei*. *J. Biol. Chem.* 278, 31988–31997.
- Ghose, T., 1987. Measurement of cellulase activities. *Pure Appl. Chem.* 59, 257–268.
- Hemsworth, G.R., Henrissat, B., Davies, G.J., Walton, P.H., 2014. Discovery and characterization of a new family of lytic polysaccharide monoxygenases. *Nat. Chem. Biol.* 10, 122–126.
- Horn, S.J., Vaaje-Kolstad, G., Westereng, B., Eijsink, V.G., 2012. Novel enzymes for the degradation of cellulose. *Biotechnol. Biofuels* 5, 45.
- Hult, E.-L., Larsson, P., Iversen, T., 2001. Cellulose fibril aggregation—an inherent property of kraft pulps. *Polymer* 42, 3309–3314.
- Igarashi, K., Uchihashi, T., Koivula, A., Wada, M., Kimura, S., Okamoto, T., Penttilä, M., Ando, T., Samejima, M., 2011. Traffic jams reduce hydrolytic efficiency of cellulase on cellulose surface. *Science* 333, 1279–1282.
- Janson, J., 1974. Analytik der polysaccharide in Holz und Zellstoff. *Faserforsch. Textiltech.* 25, 375–382.
- Karkehabadi, S., Hansson, H., Kim, S., Piens, K., Mitchinson, C., Sandgren, M., 2008. The first structure of a glycoside hydrolase FAMILY 61 member, Cel61B from *Hypocrea jecorina*, at 1.6 angstrom resolution. *J. Mol. Biol.* 383, 144–154.
- Laemmli, U.K., 1970. Cleavage of structural proteins during the assembly of the head of bacteriophage T4. *Nature* 227, 680–685.
- Larsson, P.T., Wickholm, K., Iversen, T., 1997. A CP/MAS ¹³C-NMR investigation of molecular ordering in celluloses. *Carbohydr. Res.* 302, 19–25.
- Larsson, P.T., Svensson, A., Wagberg, L., 2013. A new, robust method for measuring average fibre wall pore sizes in cellulose I rich plant fibre walls. *Cellulose* 20, 623–631.
- Lehman, L., 2011. Physiological Characterization of Enzyme Production in *Trichoderma reesei*. PhD Thesis. Technical University of Denmark.
- Liu, Y.S., Baker, J.O., Zeng, Y., Himmel, M.E., Haas, T., Ding, S.Y., 2011. Cellobiohydrolase hydrolyzes crystalline cellulose on hydrophobic faces. *J. Biol. Chem.* 286, 11195–11201.
- Lynd, L.R., Weimer, P.J., van Zyl, W.H., Pretorius, I.S., 2002. Microbial cellulose utilization: fundamentals and biotechnology. *Microbiol. Mol. Biol. Rev.* 66, 506–577 (table of contents).
- Mansfield, S.D., Mooney, C., Saddler, J.N., 1999. Substrate and enzyme characteristics that limit cellulose hydrolysis. *Biotechnol. Prog.* 15, 804–816.
- Martinez, D., Berka, R.M., Henrissat, B., Saloheimo, M., Arvas, M., Baker, S.E., Chapman, J., Chertkov, O., Coutinho, P.M., Cullen, D., Danchin, E.G., Grigoriev, I.V., Harris, P., Jackson, M., Kubicek, C.P., Han, C.S., Ho, I., Larrondo, L.F., de Leon, A.L., Magnuson, J.K., Merino, S., Misra, M., Nelson, B., Putnam, N., Robbertse, B., Salamov, A.A., Schmoll, M., Terry, A., Thayer, N., Westerholm-Parvinen, A., Schoch, C.L., Yao, J., Barabote, R., Nelson, M.A., Dettler, C., Bruce, D., Kuske, C.R., Xie, G., Richardson, P., Rokhsar, D.S., Lucas, S.M., Rubin, E.M., Dunn-Coleman, N., Ward, M., Brettin, T.S., 2008. Genome sequencing and analysis of the biomass-degrading fungus *Trichoderma reesei* (syn. *Hypocrea jecorina*). *Nat. Biotechnol.* 26, 553–560.
- Montenecourt, B.S., Eveleigh, D.E., 1977a. Preparation of mutants of *Trichoderma reesei* with enhanced cellulase production. *Appl. Environ. Microbiol.* 34, 777–782.
- Montenecourt, B.S., Eveleigh, D.E., 1977b. Semiquantitative plate assay for determination of cellulase production by *Trichoderma viride*. *Appl. Environ. Microbiol.* 33, 178–183.
- Olsson, L., Christensen, T.M.I.E., Hansen, K.P., Palmqvist, E.A., 2003. Influence of the carbon source on production of cellulases, hemicellulases and pectinases by *Trichoderma reesei* Rut C-30. *Enzyme Microb. Technol.* 33, 612–619.
- Otero, J., Panagiotou, G., Olsson, L., 2007. Fueling industrial biotechnology growth with bioethanol. In: Olsson, L. (Ed.), *Biofuels*. Springer, Berlin, Heidelberg, pp. 1–40.
- Papagianni, M., Matthey, M., Berovic, M., Kristiansen, B., 1999. *Aspergillus niger* morphology and citric acid production in submerged batch fermentation: effects of culture pH, phosphate and manganese levels. *Food Technol. Biotechnol.* 37, 165–171.
- Pauly, M., Keestra, K., 2008. Cell-wall carbohydrates and their modification as a resource for biofuels. *Plant J.* 54, 559–568.
- Percival Zhang, Y.H., Himmel, M.E., Mielenz, J.R., 2006. Outlook for cellulase improvement: screening and selection strategies. *Biotechnol. Adv.* 24, 452–481.
- Peterson, R., Nevalainen, H., 2012. *Trichoderma reesei* RUT-C30 – thirty years of strain improvement. *Microbiology* 158, 58–68.
- Qing, Q., Wyman, C.E., 2011. Supplementation with xylanase and b-xylosidase to reduce xylo-oligomer and xylan inhibition of enzymatic hydrolysis of cellulose and pretreated corn stover. *Biotechnol. Biofuels* 10, 1754–6834.
- Saloheimo, M., Paloheimo, M., Hakola, S., Pere, J., Swanson, B., Nyyssonen, E., Bhatia, A., Ward, M., Penttilä, M., 2002. Swollenin, a *Trichoderma reesei* protein with sequence similarity to the plant expansins, exhibits disruption activity on cellulosic materials. *Eur. J. Biochem.* 269, 4202–4211.
- Shcherban, T.Y., Shi, J., Durachko, D.M., Guiltinan, M.J., McQueenmason, S.J., Shieh, M., Cosgrove, D.J., 1995. Molecular cloning and sequence analysis of expansins – a highly conserved, multigene family of proteins that mediate cell wall extension in plants. *Proc. Natl. Acad. Sci. USA* 92, 9245–9249.
- Teeri, T.T., 1997. Crystalline cellulose degradation: new insight into the function of cellobiohydrolases. *Trends Biotechnol.* 15, 160–167.
- Thompson, A., Schafer, J., Kuhn, K., Kienle, S., Schwarz, J., Schmidt, G., Neumann, T., Johnstone, R., Mohammed, A.K., Hamon, C., 2003. Tandem mass tags: a novel quantification strategy for comparative analysis of complex protein mixtures by MS/MS. *Anal. Chem.* 75, 1895–1904.
- Vizcaíno, J.A., Deutsch, E.W., Wang, R., Csordas, A., Reisinger, F., Ríos, D., Dianes, J.A., Sun, Z., Farrar, T., Bandeira, N., Binz, P.A., Xenarios, I., Eisenacher, M., Mayer, G., Gatto, L., Campos, A., Chalkley, R.J., Kraus, H.J., Albar, J.P., Martinez-Bartolomé, S., Apweiler, R., Omenn, G.S., Martens, L., Jones, A.R., Hermjakob, H., 2014. ProteomeXchange provides globally coordinated proteomics data submission and dissemination. *Nat. Biotechnol.* 30, 223–226.
- Wickholm, K., Larsson, P.T., Iversen, T., 1998. Assignment of non-crystalline forms in cellulose I by CP/MAS ¹³C-NMR spectroscopy. *Carbohydr. Res.* 312, 123–129.
- Wolfenden, R., Snider, M.J., 2001. The depth of chemical time and the power of enzymes as catalysts. *Acc. Chem. Res.* 34, 938–945.
- Xiao, Z., Storms, R., Tsang, A., 2004. Microplate-based filter paper assay to measure total cellulase activity. *Biotechnol. Bioeng.* 88, 832–837.
- Yang, B., Dai, Z., Ding, S.-Y., Wyman, C.E., 2011. Enzymatic hydrolysis of cellulosic biomass. *Biofuels* 2, 421–450.
- Zhang, G., Zhu, Y., Wei, D., Wang, W., 2014. Enhanced production of heterologous proteins by the filamentous fungus *Trichoderma reesei* via disruption of the alkaline serine protease SPW combined with a pH control strategy. *Plasmid* 71, 16–22.